Asian Journal of Chemistry Vol. 20, No. 8 (2008), 6417-6434

Atomic Softness and Its Application in Site Selectivity of Antimitotic Natural Products

P.P. PANDEY, A.K. GUPTA and P.P. SINGH*
Department of Chemistry, Bareilly College, Bareilly-243 005, India
E-mail: dr_ppsingh@sify.com

The reactive sites of 19 natural product drugs having anticancer property have been identified. The site having the highest value of the descriptors except the ionization potential have been chosen as possible site through which the drug interferes with the dynamics of tubulin. The values so chosen have been used for QSAR model. 17 QSAR models have been found to have reliable predictive power. The best among them is the model obtained by using the combination of descriptors the highest softness $E_n^{\ddagger}$, the lowest ionization potential, the highest electron affinity and the highest density distribution function.

Key Words: Natural product, QSAR Model, Softness, Tubulin receptor, Atom electron density, Density distribution function.

INTRODUCTION

In nucleated cells of human body, two similar spherical proteins are found, *viz.* α-tubulin and β-tubulin, each with a molecular weight of about 50 kDa. These two proteins come together to form α-β heterodimer. Bound to these heterodimers are two molecules of guanosine triphosphate (GTP). One of these two GTP is tightly bound and cannot be removed, while the other is freely exchangeable. It is wide thought that this exchangeable GTP is intimately involved in the regulation of tubulin function[1]. The agents which interfere with the dynamics of tubulin, may also act as inhibitors of cell division. A number of inhibitors have been identified to interfere with the dynamics of tubulin and are recognized as anticancer drugs. They are divided into following categories[2]: antimetabolites, alkylating agents, natural products, antitumor antibiotics and miscellaneous agents.

We have confined the present study to the drugs of natural product category and have developed QSAR[3] models of this category of drugs using quantum chemical descriptors.

EXPERIMENTAL

The drugs of natural product group, which have been studied in this paper are the following: colchicine[4,5], steganacin[6,7], podophyllotoxin[8],

demethylpodophyllotoxin[8], deoxypodophyllotoxin[8], demethyldeoxypodo-phyllotoxin[8], α-peltatin[8], β-peltatin[8], β-peltatin A-methylether[8], combre-tastatin A-4[9,10], combretastatin A-2[11], curacin A,[12-14], 2-methoxyestradiol[15,16], centaureidin[17-19], flavonol-2[17-19], rotenone[20], griseofulvin[20], vinblastine[21], maytansine[22-24].

QSAR study is based on the following quantum chemical descriptors: atomic softness values ($E_n^{\ddagger}$, $E_m^{\ddagger}$), atom electron density (ED), ionization potential (IP), electron affinity (EA), density distribution function (DDF), average atomic softness (AAS).

The values of descriptors have been evaluated with the help of Cache-Software. The principles on which the evaluations are based are described in brief as below:

In DFT, the ground state energy of an atom or a molecule is written in terms of electron density ρ(r) and the external potential ν(r) in the form[25]

$$E(\rho) = F(\rho) + \int dr\ \rho(r)\ n(r) \quad (1)$$

where $F(\rho) = T(\rho) + V_{ee}(r)$, T(ρ) is the electronic kinetic energy functional and $V_{ee}(\rho)$ is the electron-electron interaction energy functional. The minimization of the total energy, subject to the condition that the total number of electrons is fixed,

$$N = \int dr\ \rho(r) \quad (2)$$

leads to an Euler-Lagrange equation of the form,

$$\mu = (\partial E/\delta\rho(r))_v = n(r) + \partial F/\delta\rho(r) \quad (3)$$

where μ, the Lagrange multiplier, is the chemical potential. The solution of this equation leads to the ground state density, from which one can determine the ground state energy. Parr *et al.*[25] defined the electronegativity as the negative of chemical potential, the relevant equation is given below:

$$\chi = -\mu = -(\partial E/\partial N)_v \quad (4)$$

Although the hard and soft acids and bases concept was introduced more than three decades ago by Pearson, the first unambiguous definition of hardness and softness was given by Parr and Pearson[26] in early 80s. They defined global hardness η as

$$\eta = 1/2(\delta\mu/\delta N)v_{(r)} \quad (5)$$
$$= 1/2(\delta^2E/\delta^2N)v_{(r)}$$

where E is the total energy, N the number of electrons of the chemical species and $v_{(r)}$ the external potential.

The corresponding global softness S, which bears an inverse relationship with the global hardness is defined as[27]

$$S = 1/2\eta = (\partial N/\partial\mu)v_{(r)} \quad (6)$$

The operational definition of global hardness and global softness are obtained by finite difference approximation of eqn. 1[28]

$$\eta = (IP\text{-}EA)/2 \quad (7)$$

$$S = 1/(IP\text{-}EA) \quad (8)$$

where IP and EA are the ionization potential and electron affinity respectively, of the chemical species. According to the Koopman's theorem, the IP is simply the eigen value of HOMO with change of sign and EA is the eigen value of LUMO with change of sign[29], therefore on this basis we can write

$$\eta = (\varepsilon \text{ LUMO} - \varepsilon \text{ HOMO})/2 \quad (9)$$

$$S = 1 / (\varepsilon \text{ LUMO} - \varepsilon \text{ HOMO}) \quad (10)$$

$$\chi = - (\varepsilon \text{ LUMO} + \varepsilon \text{ HOMO})/2 \quad (11)$$

$$\mu = (\varepsilon \text{ LUMO} + \varepsilon \text{ HOMO})/2 \quad (12)$$

The most important quantum mechanical framework of HSAB principle[30] was first time given by Klopman[31], who based his concept on charge and frontier orbital controlled chemical reaction and summarized the reacting species in terms of hard and soft acids and bases. For evaluation of softness values of Lewis acids and Lewis bases, he gave the following equations:

$$E_m^{\ddagger} = IP_m\text{-}a^2(IP_m\text{-}EA_m)\text{-}[\chi_r(C_r^m)^2/R_r](1\text{-}1/\in)[q_r+2b^2\chi_r(C_r^m)^2] \quad (13)$$

$$E_n^{\ddagger} = IP_n\text{-}b^2(IP_n\text{-}EA_n)\text{-}[\chi_s(C_s^n)^2/R_s](1\text{-}1/\in)[q_s\text{-}2b^2\chi_s(C_s^n)^2] \quad (14)$$

where, $E_n^{\ddagger}$ = softness of lewis acid, $E_m^{\ddagger}$ = softness of lewis base, IP = ionization potential of atom, EA = electron affinity of atom, $\in$ = dielectric constant of the medium in which reaction is carried out. R and q = Radius and charge of atom s & r, C = electron density, $\chi_r = q\text{-}(q\text{-}1)\sqrt{k}$ and k = 0.75, a & b = variational parameter defined as $a^2 + b^2 = 1$.

With the help of above equation, Klopman[31] calculated the softness value of a large number of cations and anions. Singh *et al.*[32] modified above equation and applied it to neutral species. By adopting this modified method, we have calculated the softness value of our compounds. For the solution of Klopman equation, the essential parameters are IP, EA, R, q and C, which have been evaluated on MOPAC software.

RESULTS AND DISCUSSION

The skelton structures of all compounds are shown in Figs. 1-19. Each structure has number of polar sites, through which they can interact with receptor. Such sites are indicated with each structure.

The values of ionization potential, electron affinity, atom electron density, atomic softnesses $E_n^{\ddagger}$ and $E_m^{\ddagger}$, density distribution function and average atomic softness of all the compounds at oxygen and nitrogen sites have been evaluated. For MLR analysis, the highest values of all the descriptors and the lowest value of ionization potential of each compound have been considered. Such sites of each compound are indicated at the bottom of each figure. The values of various descriptors of the above mentioned sites are included in Table-1. Outlier compounds are 13, 15 and 18.

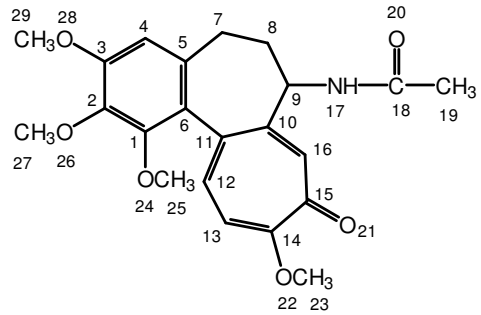

It has seven reactive sites. They are at positions 20, 21, 22, 24, 26 and 28 for six oxygen atoms and at position 17 for one nitrogen atom.

Site with the lowest IP	=	26
Site with the highest electron affinity	=	26
Site with the highest atom electron density	=	20
Site with the highest softness $E_n^{\ddagger}$	=	20
Site with the highest softness $E_m^{\ddagger}$	=	26
Site with the highest density distribution function	=	20
Site with the highest average atomic softness	=	20

Fig. 1. Structure of colchicine

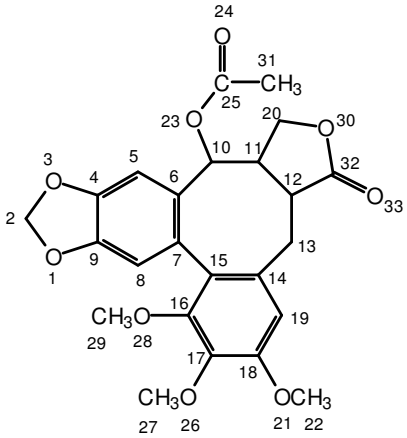

It has nine reactive sites. They are at positions 1, 3, 21, 23, 24, 26, 28, 30 and 33 for nine oxygen atoms.

Site with the lowest IP	=	26
Site with the highest electron affinity	=	26
Site with the highest atom electron density	=	23
Site with the highest softness $E_n^{\ddagger}$	=	23
Site with the highest softness $E_m^{\ddagger}$	=	26
Site with the highest density distribution function	=	23
Site with the highest average atomic softness	=	23

Fig. 2. Structure of steganacin

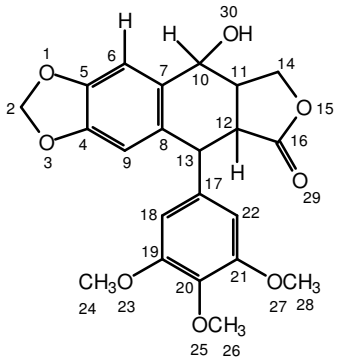

It has eight reactive sites. They are at positions 1, 3, 15, 23, 25, 27, 29 and 30 for eight oxygen atoms.

Site with the lowest IP	=	30
Site with the highest electron affinity	=	1
Site with the highest atom electron density	=	15
Site with the highest softness $E_n^{\ddagger}$	=	15
Site with the highest softness $E_m^{\ddagger}$	=	1
Site with the highest density distribution function	=	15
Site with the highest average atomic softness	=	15

Fig. 3. Structure of podophyllotoxin

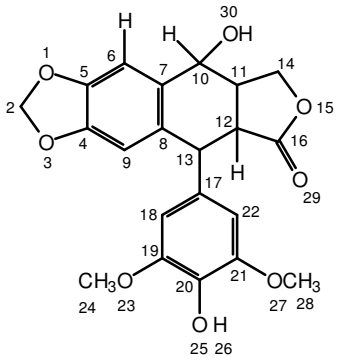

It has eight reactive sites. They are at positions 1, 3, 15, 23, 25, 27, 29 and 30 for eight oxygen atoms.

Site with the lowest IP	=	25
Site with the highest electron affinity	=	25
Site with the highest atom electron density	=	30
Site with the highest softness $E_n^{\ddagger}$	=	30
Site with the highest softness $E_m^{\ddagger}$	=	25
Site with the highest density distribution function	=	30
Site with the highest average atomic softness	=	30

Fig. 4. Structure of demethylpodophyllotoxin

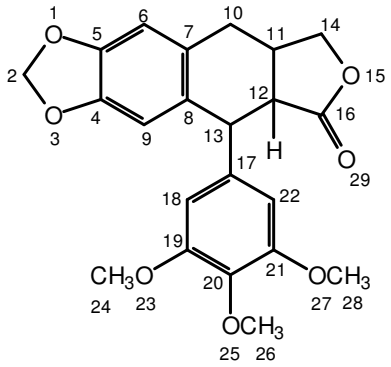

It has seven reactive sites. They are at positions 1, 3, 15, 23, 25, 27 and 29 for seven oxygen atoms.

Site with the lowest IP	=	25
Site with the highest electron affinity	=	25
Site with the highest atom electron density	=	15
Site with the highest softness $E_n^{\ddagger}$	=	15
Site with the highest softness $E_m^{\ddagger}$	=	25
Site with the highest density distribution function	=	15
Site with the highest average atomic softness	=	15

Fig. 5. Structure of deoxypodophyllotoxin

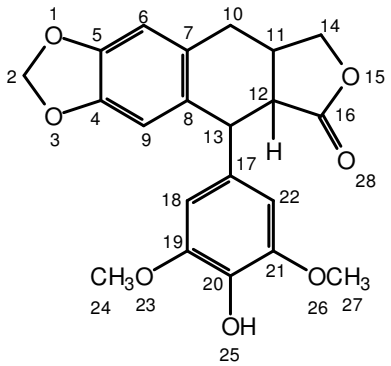

It has seven reactive sites. They are at positions 1, 3, 15, 23, 25, 26 and 28 for seven oxygen atoms.

Site with the lowest IP	=	1
Site with the highest electron affinity	=	1
Site with the highest atom electron density	=	15
Site with the highest softness $E_n^{\ddagger}$	=	15
Site with the highest softness $E_m^{\ddagger}$	=	1
Site with the highest density distribution function	=	15
Site with the highest average atomic softness	=	15

Fig. 6. Structure of demethoxypodophyllotoxin

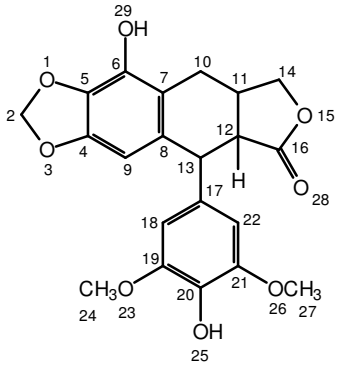

It has eight reactive sites. They are at positions 1, 3, 15, 23, 25, 26, 28 and 29 for eight oxygen atoms

Site with the lowest IP	=	1
Site with the highest electron affinity	=	1
Site with the highest atom electron density	=	28
Site with the highest softness $E_n^{\ddagger}$	=	28
Site with the highest softness $E_m^{\ddagger}$	=	1
Site with the highest density distribution function	=	28
Site with the highest average atomic softness	=	28

Fig. 7. Structure of α-peltatin

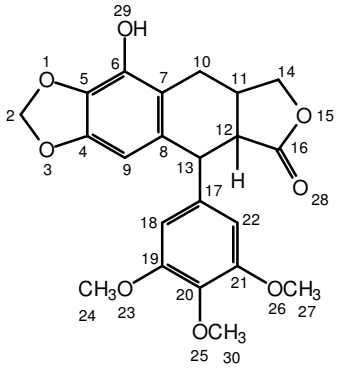

It has seven reactive sites. They are at positions 1, 3, 15, 23, 25, 26 and 28 for seven oxygen atoms.

Site with the lowest IP	=	1
Site with the highest electron affinity	=	1
Site with the highest atom electron density	=	15
Site with the highest softness $E_n^{\ddagger}$	=	15
Site with the highest softness $E_m^{\ddagger}$	=	1
Site with the highest density distribution function	=	15
Site with the highest average atomic softness	=	15

Fig. 8. Structure of β-peltatin

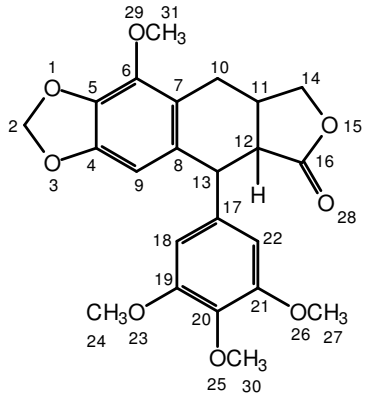

It has eight reactive sites. They are at positions 1, 3, 15, 23, 25, 26, 28 and 29 for eight oxygen atoms

Site with the lowest IP	=	25
Site with the highest electron affinity	=	25
Site with the highest atom electron density	=	28
Site with the highest softness $E_n^{\ddagger}$	=	28
Site with the highest softness $E_m^{\ddagger}$	=	25
Site with the highest density distribution function	=	28
Site with the highest average atomic softness	=	28

Fig. 9. Structure of β-peltatin A-methylether

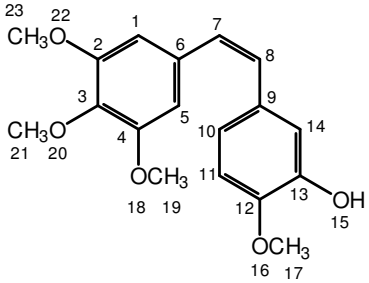

It has five reactive sites. They are at positions 15, 16, 18, 20 and 22 for five oxygen atoms.

Site with the lowest IP	=	16
Site with the highest electron affinity	=	16
Site with the highest atom electron density	=	22
Site with the highest softness $E_n^{\ddagger}$	=	22
Site with the highest softness $E_m^{\ddagger}$	=	16
Site with the highest density distribution function	=	22
Site with the highest average atomic softness	=	22

Fig. 10. Structure of combretastatin A-4

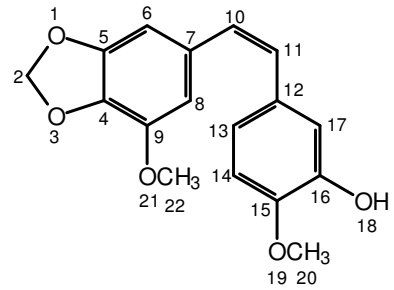

It has five reactive sites. They are at positions 1, 3, 18, 19 and 21 for five oxygen atoms.

Site with the lowest IP	=	19
Site with the highest electron affinity	=	19
Site with the highest atom electron density	=	18
Site with the highest softness $E_n^{\ddagger}$	=	18
Site with the highest softness $E_m^{\ddagger}$	=	19
Site with the highest density distribution function	=	18
Site with the highest average atomic softness	=	18

Fig. 11. Structure of combretastatin A-2

TABLE-1
VALUES OF DESCRIPTORS BASED ON ATOMIC PROPERTIES OF ALL THE COMPOUNDS

Compd.	Highest $E_n^{\ddagger}$	Highest $E_m^{\ddagger}$	Highest atom electron density	Lowest ionization potential	Highest electron affinity	Highest density distribution function	Highest average atomic softness	Activity (log P)
1	257.114	-9.094	6.279	13.193	-2.294	43.225	27.979	0.944
2	249.253	-4.614	6.197	10.610	2.325	42.661	27.119	1.673
3	247.066	-11.437	6.173	16.237	-2.414	42.496	27.119	1.408
4	249.685	-10.844	6.198	16.109	-1.853	42.668	27.180	1.654
5	246.244	-7.503	6.166	13.216	0.397	42.447	27.073	2.276
6	246.220	-11.552	6.166	16.264	-2.748	42.447	27.074	2.244
7	251.962	-11.330	6.222	16.109	-2.567	42.833	27.297	1.960
8	251.591	-7.739	6.218	13.439	0.252	42.805	27.289	1.992
9	246.883	-7.440	6.172	13.216	0.489	42.489	27.278	2.023
10	248.876	-7.212	6.199	11.421	-0.813	42.675	27.074	1.096
11	255.865	-9.748	6.262	14.532	-1.707	43.108	27.380	2.808
12	131.400	10.208	5.205	3.792	19.704	68.231	15.251	6.372
14	255.739	-11.970	6.263	15.755	-3.842	43.115	27.418	0.090
16	255.978	-10.511	6.270	13.663	-3.644	43.163	27.713	2.426
17	251.355	-8.589	6.213	14.666	0.127	42.771	27.170	0.156
19	305.463	-5.472	6.926	12.370	0.320	85.337	31.212	3.500

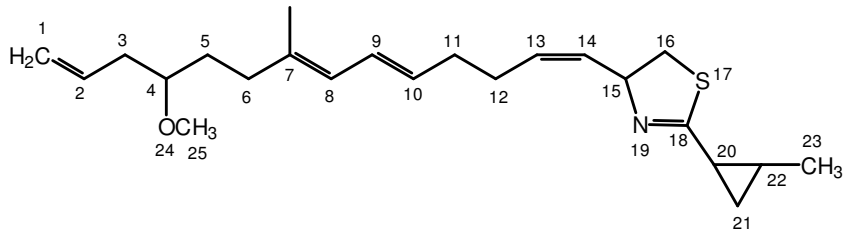

It has three reactive sites. They are at positions 17 for one sulphur atom, 19 for one nitrogen atom and 24 for one oxygen atom.

Site with the lowest IP	=	17
Site with the highest electron affinity	=	17
Site with the highest atom electron density	=	24
Site with the highest softness $E_n^{\ddagger}$	=	24
Site with the highest softness $E_m^{\ddagger}$	=	17
Site with the highest density distribution function	=	17
Site with the highest average atomic softness	=	24

Fig. 12. Structure of curacin A

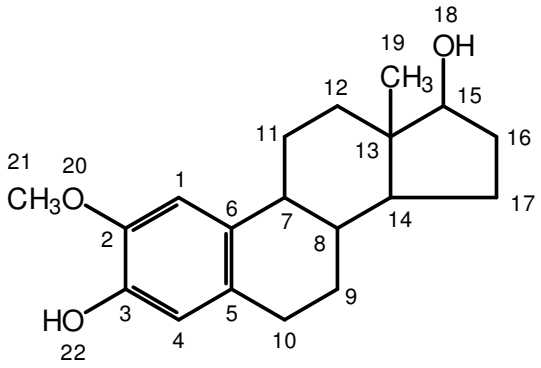

It has three reactive sites. They are at positions 18, 20 and 22 for three oxygen atoms

Site with the lowest IP	=	22
Site with the highest electron affinity	=	22
Site with the highest atom electron density	=	20
Site with the highest softness $E_n^{\ddagger}$	=	20
Site with the highest softness $E_m^{\ddagger}$	=	22
Site with the highest density distribution function	=	20
Site with the highest average atomic softness	=	20

Fig. 13. Structure of 2-methoxyestradiol

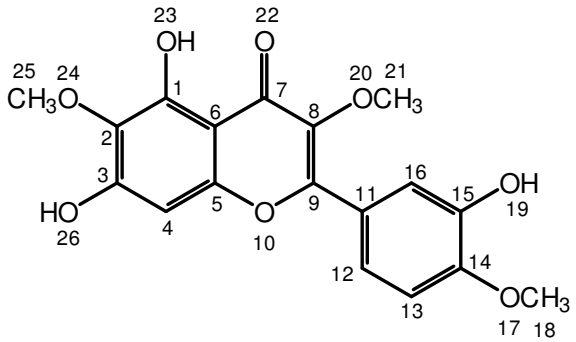

It has eight reactive sites. They are at positions 10, 17, 19, 20, 22, 23, 24 and 26 for eight oxygen atoms.

Site with the lowest IP	=	19
Site with the highest electron affinity	=	19
Site with the highest atom electron density	=	10
Site with the highest softness $E_n^{\ddagger}$	=	10
Site with the highest softness $E_m^{\ddagger}$	=	19
Site with the highest density distribution function	=	10
Site with the highest average atomic softness	=	10

Fig. 14. Structure of centaureidin

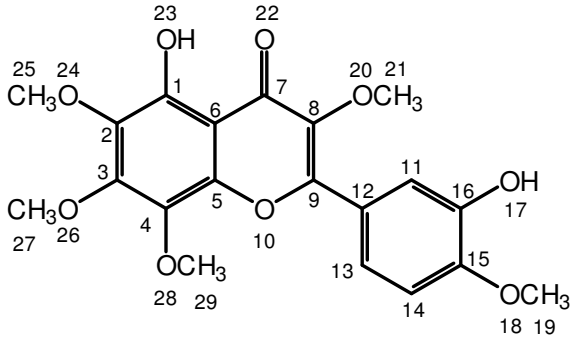

It has nine reactive sites. They are at positions 10, 17, 18, 20, 22, 23, 24, 26 and 28 for nine oxygen atoms.

Site with the lowest IP	=	22
Site with the highest electron affinity	=	22
Site with the highest atom electron density	=	18
Site with the highest softness $E_n^{\ddagger}$	=	18
Site with the highest softness $E_m^{\ddagger}$	=	22
Site with the highest density distribution function	=	18
Site with the highest average atomic softness	=	18

Fig. 15. Structure of flavonol-2

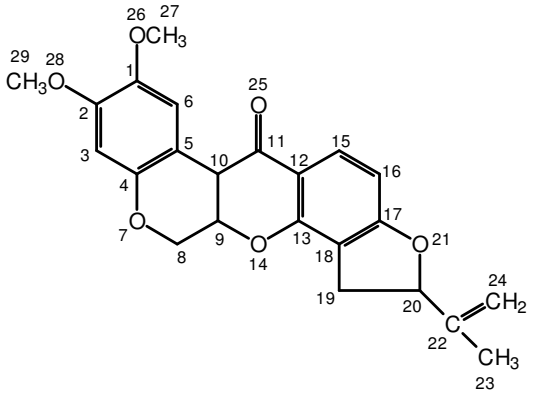

It has six reactive sites. They are at positions 7, 14, 21, 25, 26 and 28 for six oxygen atoms.

Site with the lowest IP	=	7
Site with the highest electron affinity	=	7
Site with the highest atom electron density	=	25
Site with the highest softness $E_n^{\ddagger}$	=	25
Site with the highest softness $E_m^{\ddagger}$	=	7
Site with the highest density distribution function	=	25
Site with the highest average atomic softness	=	25

Fig. 16. Structure of rotenone

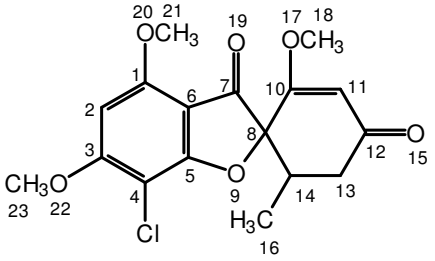

It has seven reactive sites. They are at positions 9, 15, 17, 19, 20 and 22 for six oxygen atoms and 24 for one chlorine atom.

Site with the lowest IP	=	9
Site with the highest electron affinity	=	9
Site with the highest atom electron density	=	19
Site with the highest softness $E_n^{\ddagger}$	=	19
Site with the highest softness $E_m^{\ddagger}$	=	9
Site with the highest density distribution function	=	19
Site with the highest average atomic softness	=	19

Fig. 17. Structure of griseofulvin

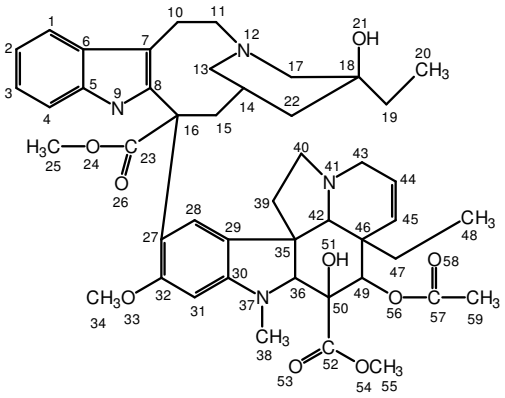

It has thirteen reactive sites. They are at positions 9, 12, 37 and 41 for four nitrogen atoms and 21, 24, 26, 33, 51, 53, 54, 56 and 58 for nine oxygen atoms.

Site with the lowest IP	=	26
Site with the highest electron affinity	=	26
Site with the highest atom electron density	=	53
Site with the highest softness $E_n^{\ddagger}$	=	53
Site with the highest softness $E_m^{\ddagger}$	=	26
Site with the highest density distribution function	=	53
Site with the highest average atomic softness	=	53

Fig. 18. Structure of vinblastine

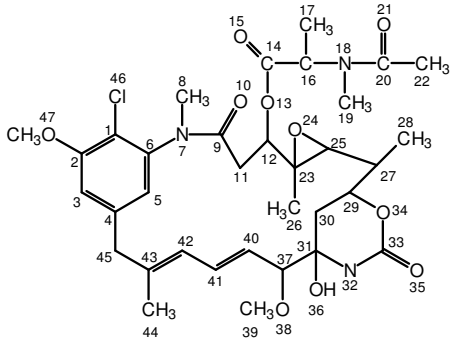

It has fourteen reactive sites. They are at positions 7, 18 and 32 for three nitrogen atoms, 10, 13, 15, 21, 24, 34, 35, 36, 38 and 47 for ten oxygen atoms and 46 for one chlorine atom.

Site with the lowest IP	=	46
Site with the highest electron affinity	=	46
Site with the highest atom electron density	=	46
Site with the highest softness $E_n^{\ddagger}$	=	46
Site with the highest softness $E_m^{\ddagger}$	=	46
Site with the highest density distribution function	=	46
Site with the highest average atomic softness	=	46

Fig. 19. Structure of rotenone

QSAR Models

90 Regression equations using various combinations of quantum chemical descriptors have been tried for QSAR models. But only 17 models have been found successful because their correlation coefficients are greater than 0.5. Such equations are presented below:

1. APA1 = -0.0240554 * $E_n^{\ddagger}$ + 0.07438 * DDF + 4.48064
   rCV^2 = 0.351488, r^2 = 0.738049
2. APA2 = 0.212125 * $E_m^{\ddagger}$ -0.00551537 * IP + 3.76558
   rCV^2 = 0.353077, r^2 = 0.621342
3. APA3 = 0.0325936 * $E_m^{\ddagger}$ + 0.180591 * EA + 2.28202
   rCV^2 = 0.249041, r^2 = 0.638048
4. APA4 = -2.54856 * ED + 0.0862621 * DDF + 13.7719
   rCV^2 = 0.282514, r^2 = 0.737884
5. APA5 = -0.0235093 * IP + 0.191554 * EA + 2.33147
   rCV^2 = 0.578439, r^2 = 0.637947
6. APA6 = -0.170296 * $E_n^{\ddagger}$ + 0.00675055 * $E_m^{\ddagger}$ + 15.5792* ED-52.3813
   rCV^2 = 0.182078, r^2 = 0.737642
7. APA7 = -0.0231529 * $E_n^{\ddagger}$ + 0.00794681 * $E_m^{\ddagger}$ + 0.0725263 * DDF + 4.40697
   rCV^2 = 0.413959, r^2 = 0.738163
8. APA8 = 0.00862153 * $E_m^{\ddagger}$ - 2.44486 * ED + 0.0837676 * DDF+ 13.314
   rCV^2 = 0.269098, r^2 = 0.738019
9. APA9 = -2.38403 * ED-0.014157 * IP + 0.0828649 * DDF + 13.0956
   rCV^2 = 0.32925, r^2 = 0.738175
10. APA10 = -2.06231*ED + 0.0344782 * EA + 0.076849* DDF + 11.1998
    rCV^2 = 0.269851, r^2 = 0.739112
11. APA11 = -0.0227732* $E_n^{\ddagger}$ -0.0116615*IP + 0.0722141*DDF+4.41692
    rCV^2 = 0.34578, r^2 = 0.738242
12. APA12 = -0.0194249* $E_n^{\ddagger}$ + 0.0348209*EA+0.0671619*DDF+3.67457
    rCV^2 = 0.362717, r^2 = 0.739319
13. APA13 = -2.05844* ED+ 0.01328* IP+ 0.045698*EA+ 0.0769732* DDF + 10.9973
    rCV^2 = 0.406341, r^2 = 0.739238
14. APA14 = -0.0194431* $E_n^{\ddagger}$ + 0.0186107 * IP + 0.0500722*EA + 0.0674571*DDF + 3.4232
    rCV^2 = 0.29086, r^2 = 0.739567
15. APA15 = 0.217049 * $E_m^{\ddagger}$ + 3.73258
    rCV^2 = 0.507772, r^2 = 0.621332
16. APA16 = -0.235693 * IP + 5.09135
    rCV^2 = 0.488278, r^2 = 0.602868
17. APA17 = 0.211356 * EA + 2.02577
    rCV^2 = 0.605935, r^2 = 0.637545

The predicted activities, derived from the above seventeen regression equations, are presented in Tables 2 and 3.

TABLE-2
PREDICTED ACTIVITIES APA1 TO APA9 OF THE COMPOUNDS

Compd.	APA1	APA2	APA3	APA4	APA5	APA6	APA7	APA8	APA9
1	1.511	1.764	1.571	1.498	1.582	1.594	1.517	1.505	1.521
2	1.658	2.728	2.552	1.658	2.527	1.685	1.693	1.697	1.707
3	1.698	1.249	1.473	1.705	1.483	1.638	1.678	1.683	1.668
4	1.648	1.376	1.594	1.657	1.598	1.585	1.634	1.641	1.627
5	1.714	2.101	2.109	1.719	2.097	1.695	1.725	1.730	1.726
6	1.715	1.225	1.409	1.719	1.423	1.672	1.693	1.695	1.683
7	1.605	1.273	1.449	1.610	1.461	1.568	1.590	1.592	1.583
8	1.612	2.050	2.075	1.617	2.064	1.593	1.625	1.631	1.628
9	1.702	2.114	2.128	1.707	2.114	1.680	1.713	1.719	1.715
10	1.668	2.173	1.900	1.655	1.907	1.763	1.683	1.671	1.692
11	1.532	1.618	1.656	1.531	1.663	1.537	1.532	1.531	1.533
12	6.395	5.952	6.173	6.392	6.195	6.401	6.394	6.392	6.394
14	1.536	1.140	1.198	1.529	1.225	1.559	1.518	1.510	1.514
16	1.533	1.461	1.281	1.516	1.312	1.638	1.527	1.510	1.531
17	1.615	1.863	1.892	1.627	1.870	1.550	1.621	1.633	1.620
19	3.480	2.537	2.161	3.482	2.102	3.464	3.480	3.482	3.480

TABLE-3
PREDICTED ACTIVITIES APA10 TO APA17 OF THE COMPOUNDS

Compd.	APA10	APA11	APA12	APA13	APA14	APA15	APA16	APA17
1	1.493	1.529	1.503	1.470	1.471	1.759	1.982	1.541
2	1.778	1.698	1.779	1.772	1.769	2.731	2.591	2.517
3	1.652	1.668	1.645	1.670	1.671	1.250	1.216	1.516
4	1.633	1.624	1.626	1.653	1.654	1.379	1.295	1.634
5	1.759	1.720	1.756	1.766	1.765	2.104	1.976	2.110
6	1.651	1.685	1.647	1.663	1.664	1.225	1.258	1.445
7	1.571	1.584	1.568	1.583	1.585	1.273	1.295	1.483
8	1.675	1.622	1.671	1.683	1.682	2.053	1.924	2.079
9	1.753	1.709	1.750	1.761	1.760	2.118	1.976	2.129
10	1.667	1.698	1.678	1.636	1.635	2.167	2.400	1.854
11	1.540	1.534	1.540	1.540	1.541	1.617	1.666	1.665
12	6.388	6.396	6.391	6.385	6.387	5.948	5.985	6.190
14	1.464	1.523	1.469	1.458	1.460	1.134	1.378	1.214
16	1.461	1.545	1.474	1.428	1.430	1.451	1.871	1.256
17	1.653	1.610	1.643	1.667	1.664	1.868	1.635	1.897
19	3.485	3.479	3.484	3.488	3.487	2.545	2.176	2.093

Regression equations in which cross-validation coefficient (rCV^2) is greater than 0.2 and regression coefficient (r^2) is greater than 0.5 has good predictive power. The values of cross-validation coefficients and regression coefficients of these predicted activities are listed in the Table-4.

TABLE-4
VALUES OF CROSS-VALIDATION COEFFICIENTS AND REGRESSION COEFFICIENTS OF THE PREDICTED ACTIVITIES HAVING GOOD PREDICTIVE POWER IN DECREASING ORDER OF PREDICTIVE POWER

Predicted activity	Cross-validation coefficient (rCV^2)	Regression coefficient (r^2)
APA14	0.290860	0.739567
APA12	0.362717	0.739319
APA13	0.406341	0.739238
APA10	0.269851	0.739112
APA11	0.345780	0.738242
APA9	0.329250	0.738175
APA7	0.413959	0.738163
APA1	0.351488	0.738049
APA8	0.269098	0.738019
APA4	0.282514	0.737884
APA6	0.182078	0.737642
APA3	0.249041	0.638048
APA5	0.578439	0.637947
APA17	0.605935	0.637545
APA2	0.353077	0.621342
APA15	0.507772	0.621332
APA16	0.488278	0.602868

It is clear from the Table-4 that the predicted activity APA14 obtained by using the combination of descriptors highest softness $E_n^{\ddagger}$, lowest ionization potential, highest electron affinity and highest density distribution function has highest predictive power. Observed activity in terms of log P and the predicted activity APA14 are given in Fig. 20.

Next highest predictive power is in the predictive activity APA12 obtained by using the combination of descriptors softness $E_n^{\ddagger}$, electron affinity and density distribution function. Observed activity in terms of log P and the predicted activity APA12 are given in Fig. 21.

Next highest predictive power is in the predictive activity APA13 obtained by using the combination of descriptors atom electron density, ionization potential, electron affinity and density distribution function. Observed activity in terms of log P and the predicted activity APA13 are

given in Fig. 22.

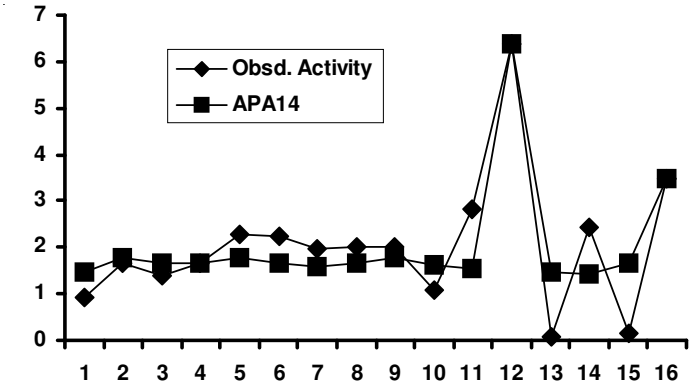

Fig. 20. Graph between observed activity and the predicted activity APA14

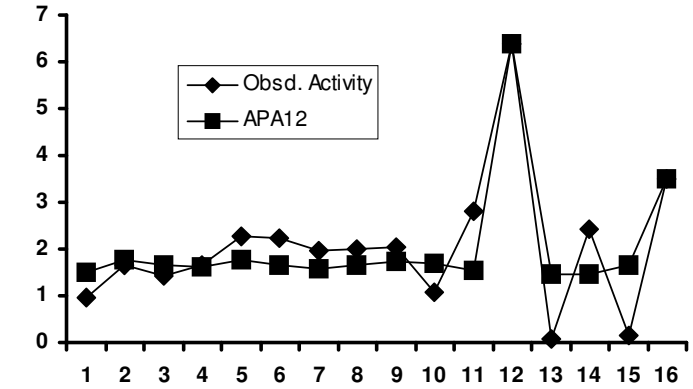

Fig. 21. Graph between observed activity and the predicted activity APA12

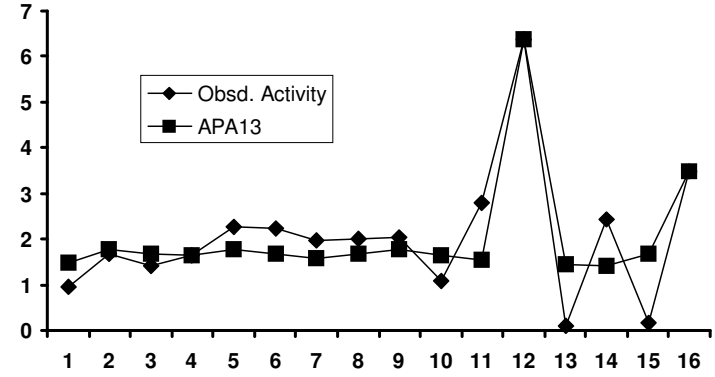

Fig. 22. Graph between observed activity and the predicted activity APA13

REFERENCES

1. A. Jordan, J.A. Hadfield, N.J. Lawrence and A.T. McGown, *Med. Res. Rev.*, **18**, 259 (1998).
2. G.L. Coppoc, Pharmacology of Cancer Therapy, Purduc Research Foundation (1996).
3. C. Hansch and C. Silipo, *J. Med. Chem.*, **17**, 661 (1974).
4. S.B. Hastie, *Pharmac. Ther.*, **51**, 377 (1991).
5. O. Boye and A. Brossi, *Alkaloids*, **41**, 125 (1992).
6. M.S. Kupchan, R.W. Britton, M.F. Ziegler, C.J. Gilmore, R.J. Restivo and R.F. Bryan, *J. Am. Chem. Soc.*, **95**, 1335 (1973).
7. P.B. Schiff, A.S. Kende, S.B. Horwitz, *Biochem. Biophys. Res. Commun.*, **85**, 737 (1978).
8. D.L. Sackett, *Pharmac. Ther.*, **59**, 163 (1993).
9. G.R. Pettit, G.M. Cragg, D.L. Herald, J.M. Schmidt and P. Lohavanijaya, *Can. J. Chem.*, **60**, 1374 (1982).
10. G.R. Pettit, S.B. Singh, E. Hamel, C.M. Lin and D.S. Alberts, *Experientia*, **45**, 209 (1989).
11. G.R. Pettit and S.B. Singh, *Can. J. Chem.*, **65**, 2390 (1987).
12. W.H. Gerwick, P.J. Proteau, D.G. Nagle, E. Hamel, A. Blokhin and D.L. Slate, *J. Org. Chem.*, **59**, 1243 (1994).
13. D.G. Nagle, R.S. Geralds, H.D. Yoo, W.H. Gerwick, T.S. Kim, M. Nambu and J.D. White, *Tetrahedron Lett.*, **36**, 1189 (1995).
14. A.V. Blokhin, H.D. Yoo, R.S. Geralds, D.G. Nagle, W.H. Gerwick and E. Hamel, *Mol. Pharmacol.*, **48**, 523 (1995).
15. D. Berg, R. Sonsalla and E. Kuss, *Acta Endocrin.*, **103**, 282 (1983).
16. R.J. D' Amato, C.M. Lin, E. Flynn, J. Folkman and E. Hamel, *Proc. Natl. Acad. Sci. (USA)*, **91**, 3964 (1994).
17. J.A. Beutler, J.H. Cardellina II, C.M. Lin, E. Hamel, G.M. Cragg and M.R. Boyd, *Med. Chem. Lett.*, **3**, 581 (1993).
18. J.J. Lichius, O. Thoison, A. Montagnae, M. Pais, F. Gueritte-Voegelein and T. Sevenet, *J. Nat. Prod.*, **57**, 1012 (1994).
19. Q. Shi, K. Chen, L. Li, J.J. Chang, C. Autry, M. Kozuka, T. Konoshima, J.R. Estes, C.M. Li, E. Hamel, A.T. McPhail, D.R. McPhail and K.H. Lee, *J. Nat. Prod.*, **58**, 475 (1995).
20. E. Hamel, in ed.: J. Avila, Microtubule Proteins, CRC Press, Boca Rotan, FL, p. 89 (1990).
21. R.H. Himes, *Pharmac. Ther.*, **51**, 257 (1991).
22. E. Hamel, *Pharmac. Ther.*, **55**, 31 (1992).
23. S.M. Kupchan, Y. Komoda, W.A. Court, G.J. Thomas, R.M. Smith, A. Kariro, C.J. Gilmore, R.C. Haltiwanger and R.F. Bryan, *J. Am. Chem. Soc.*, **94**, 1354 (1972).
24. M. Asai, E. Mizuta, M. Izawa, K. Haibara and T. Kishi, *Tetrahedron*, **35**, 1079 (1979).
25. R.G. Parr and W. Yang, Density-Functional Theory of Atoms and Molecules, Oxford University Press (1994).
26. R.G. Parr and R.G. Pearson, *J. Am. Chem. Soc.*, **105**, 7512 (1983).
27. W. Yang and R.G. Parr, *Proc. Natl. Acad. Sci. (USA)*, **82**, 6723 (1985).
28. F. De Proft, W. Langenaeker and P. Geerlings, *J. Phys. Chem.*, **97**, 1826 (1993).
29. R.G. Pearson, *Acc. Chem. Res.*, **26**, 250 (1993).
30. R.G. Pearson, Hard and Soft Acid and Bases, Stroudsville, PA, Dowden, Hutchinson And Ross (1973).
31. G. Klopman, *J. Am. Chem. Soc.*, **90**, 223 (1968).
32. P.P. Singh, S.K. Srivastava and A.K. Srivastava, *J. Inorg. Nucl. Chem.*, **42**, 5212 (1980).

(*Received*: 13 February 2008; *Accepted*: 14 July 2008) AJC-6700